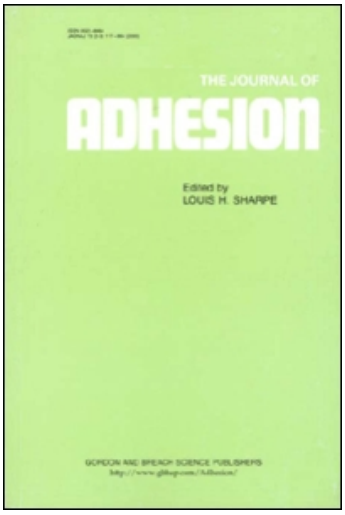

The Journal of Adhesion
Publication details, including instructions for authors and subscription information:
http://www.informaworld.com/smpp/title~content=t713453635

Effect of Boron Carbide Filler on the Curing and Mechanical Properties of an Epoxy Resin

J. Abenojar[a]; M. A. Martínez[a]; F. Velasco[a]; V. Pascual-Sánchez[b]; J. M. Martín-Martínez[b]
[a] Department of Materials Science and Engineering, University Carlos III of Madrid, Leganés, Spain [b] Adhesion and Adhesives Laboratory, University of Alicante, Alicante, Spain

To cite this Article Abenojar, J. , Martínez, M. A. , Velasco, F. , Pascual-Sánchez, V. and Martín-Martínez, J. M.(2009) 'Effect of Boron Carbide Filler on the Curing and Mechanical Properties of an Epoxy Resin', The Journal of Adhesion, 85: 4, 216 — 238
To link to this Article: DOI: 10.1080/00218460902881782
URL: http://dx.doi.org/10.1080/00218460902881782

The Journal of Adhesion, 85:216–238, 2009

ISSN: 0021-8464 print/1545-5823 online
DOI: 10.1080/00218460902881782

Taylor & Francis
Taylor & Francis Group

Effect of Boron Carbide Filler on the Curing and Mechanical Properties of an Epoxy Resin

J. Abenojar[1], M. A. Martínez[1], F. Velasco[1], V. Pascual-Sánchez[2], and J. M. Martín-Martínez[2]
[1]Department of Materials Science and Engineering, University Carlos III of Madrid, Leganés, Spain
[2]Adhesion and Adhesives Laboratory, University of Alicante, Alicante, Spain

The curing process, wear behavior, and mechanical properties of an epoxy adhesive filled with boron carbide (B_4C) were studied. Two different particle sizes and amount of reinforcing B_4C were tested. One advantage of using B_4C is its ability to absorb neutrons, a property of great importance in the nuclear industry. Gel time and degree of curing were measured to evaluate the effect of adding B_4C to the epoxy resin. The chemical structure was studied by Fourier Transform Infrared Spectroscopy (FTIR) and the B_4C distribution was analyzed by laser confocal microscopy. Dynamic Mechanical Thermal Analysis (DMTA) tests were also carried out to monitor the viscoelastic properties and the glass transition temperature (T_g) of the cured reinforced epoxy. The wear resistance against alumina was measured using a pin-on-disc test, evaluated as mass loss. The wear tracks were studied by Scanning Electron Microscopy (SEM). The bending strength was also studied to assess the degree of interaction between the B_4C and the matrix. The results showed that the reinforced epoxy with B_4C was very abrasive, wearing the alumina. The reinforced epoxy had excellent mechanical properties that increased with B_4C content and with small particles. Moreover, the T_g value decreased slightly upon B_4C addition.

Keywords: Boron carbide; DMTA; Epoxy; Filler; Mechanical properties; Wear resistance

Received 14 July 2008; in final form 19 December 2008.
Presented in part at the 2nd International Conference on Advanced Computational Engineering and Experimenting (ACE-X 2008), Barcelona, Spain, 14–15, July 2008.
Address correspondence to J. Abenojar, Department of Materials Science and Engineering, University Carlos III of Madrid, 28911 Leganés, Spain. E-mail: abenojar@ing.uc3.es

1. INTRODUCTION

The reinforcement in a polymer matrix composite (PMC) increases the strength and stiffness of the relatively weak matrix. The function of the matrix is to bond the reinforcements together and transmit the loads between them.

Polymeric materials are being increasingly used in a wide variety of applications in which wear resistance is important. Polymers are ideal for applications where their general resistance to corrosion, galling, and seizure, their tolerance to small misalignments, and shock loading are necessary, *e.g.*, bearings. Their low density and high toughness are desirable properties. In many applications, polymers can be subjected to abrasive wear, often due to the presence of contaminants, and such abrasion may result in loss of function.

Epoxy resins are widely used in the industry, being one of the most applied materials as matrix in composite materials, due to their excellent adhesion to different reinforcements and their slight shrinkage during the curing process. Their low viscosity, high hardness, and good resistance to humidity and fatigue must also be highlighted. They are also used in the atomic energy field, *e.g.*, floor painting in radiation facilities and for nuclear fuel casks, as they have good durability to gamma rays [1]. Moreover, epoxy resins show excellent durability to reactor neutrons with a degassing character and form stability.

Epoxy resins require a curing process to be crosslinked and produce polymers with three-dimensional and insoluble networks. The final properties of the cured epoxy arise from the nature of the epoxy resin and curing agent, the curing cycle, degree of conversion, and degree of crosslinking among other factors [2].

On the other hand, the properties of the composite depend on the matrix, reinforcement, and the interface between them. The matrix must transfer the applied load to the reinforcement. The reinforcement, depending on volume, size, shape, and nature can affect many properties including strength, hardness, wear resistance, heat dissipation, and dimensional stability. However, one of the key issues is finding the optimal ratio between polymer matrix and filler to yield materials with the desired range of properties for a specific application.

Boron carbide (B_4C) ceramics and composites are important high-tech materials, mainly due to their high level of hardness and low density [3]. Specifically, B_4C is the third hardest material after diamond and cubic boron nitride [4]. One of the major uses of B_4C is as an abrasive. Different authors have studied B_4C wear, with and

without additives [5,6]. The influence of particle properties on the erosive wear of sintered boron carbide has also been studied [7]. It was found that different erodents (silica, alumina, silicon carbide) cause different erosion mechanisms. B_4C also presents a high melting point and high neutron absorption cross-section [8,9]. Despite being a neutron absorber material, it does not detect luminescence intensity at low temperatures (below 5 K) and it is opaque to visible light [10]. Its behavior is similar to other weak neutron absorber materials such as acrylic or tetraphenyl butadiene (TPB) evaporated on Gore-Tex®.

Few researches deal with B_4C reinforced polymer matrix composites (PMCs). B_4C has been used with polyethylene at a concentration of 2 wt.%, improving the radiation shielding properties of the neat polyethylene [11]. B_4C-epoxy composites serve as components of the neutron shield for the fission residues located outside the cavity of a nuclear reactor, likewise preventing neutrons from escaping and creating a time-dependent background [12]. Also, epoxy resin mixed with neutron shielding materials (including B_4C) have been used for several components of neutron spectrometer construction [13], such as shielding blocks, bricks, beam narrowers, and stoppers.

To our knowledge, a systematic study dealing with the use of B_4C as filler of epoxy resin has not been performed. Therefore, the main objective of this study is the addition of different amounts of two different boron carbide fillers with different particle size to epoxy resin, and to specifically analyze the effects of their addition on the curing and mechanical properties of the filled epoxy materials.

2. EXPERIMENTAL DETAILS

2.1. Materials

The epoxy used was Hysol 9483, supplied by Henkel Adhesivos y Tecnologías S.L. (Navalcarnero, Madrid, Spain) [14]. It shows low viscosity (7 Pa · s), high mechanical strength (UTS of 47 N/mm^2 according to the manufacturer), and it cures at room temperature during 12 h. The epoxy resin was 4,4′-isopropylidendiphenol-based and the hardener was 4,7,10-trioxa-1,13-tridecanediamine-based. The mix ratio (by wt.) resin:hardener was 100:46.

Two different B_4C particle sizes were used: one with an average particle size of 7 μm (Fig. 1a), supplied by Strem Chemicals (Bischheim, France), and the other with 23 μm (Fig. 1b), supplied by Presi (Grenoble, France). Both of them have high purity (more than 99%). The morphology of the particles was analysed by scanning electron microscopy (Philips XL 30, FEI Europa, Eindhoven,

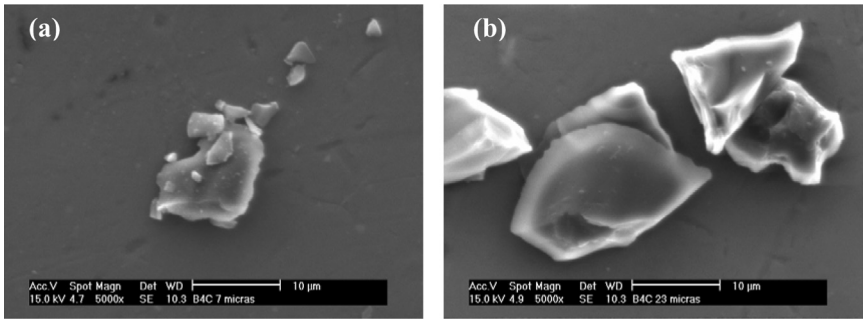

FIGURE 1 SEM microstructures of B_4C particles: (a) 7 μm and (b) 23 μm.

Netherlands). The particles have a polygonal shape with sharp edges (Fig. 1). No surface treatment was applied to the B_4C particles.

The particles were added to the resin in two different amounts, 6 and 12% (by wt.). It is important to adequately disperse particles in the polymer without producing their agglomeration, in particular when adding nano-particles [15,16]. The mechanical agitation method was used in this case, maintaining the same high-speed shearing force constant during an approximate period of 5 min. The mixture was subsequently poured into silicone (Silastic 3481, Feroca, Madrid, Spain) molds to obtain the desired test specimen form ($30 \times 12.5 \times 2\,mm^3$). The five studied materials are summarized in Table 1.

2.2. Experimental Techniques

2.2.1. Infrared Spectroscopy

The cure kinetics and the degree of conversion of the materials were monitored by using a Bruker Vector 22 (Ettlingen, Germany) infrared spectrometer, fitted with transformed Fourier (FTIR) analysis.

TABLE 1 Composition and Abbreviation of the Studied Materials

	Reinforcement (B_4C)		
Epoxy resin	% weight	Particle size (μm)	Sample reference
Hysol 9483			H
Hysol 9483	6	7	H6C7
Hysol 9483	12	7	H12C7
Hysol 9483	6	23	H6C23
Hysol 9483	12	23	H12C23

The FTIR spectra of the composites used in this study were obtained by means of "transmission in film," depositing a small drop of the materials on a potassium bromide (KBr) window, and carefully spreading it with a spatula to obtain a thin film. It was then placed in the sample holder of the spectrometer in such a way that the infrared spectroscopy beam crossed it perpendicularly. A total of 60 scans were carried out for each infrared spectrum with a resolution of $4\,cm^{-1}$.

It was possible to follow the temporary evolution of the concentration level of the species involved in the curing process of the epoxy resins, as well as the conversion percentage. Consecutive infrared spectra were measured to follow the curing kinetics of the epoxy resin-hardener mixture. Measurement were carried out every 15 min for 15 h. To quantify the cure kinetics and degree of conversion (α) of the filled epoxy with time (t), the ratio of the areas of the bands at $1035\,cm^{-1}$ (characteristic of the stretching of the C-H in the aromatic ring of the bisphenol, $Abs_{1035\,cm^{-1}}$) and $915\,cm^{-1}$ (characteristic of the oxirane group in the epoxy ring, $Abs_{915\,cm^{-1}}$) were chosen [(Eq. (1)]. The curing produced the disappearance of the oxirane at $915\,cm^{-1}$, so it was used to quantify the degree of conversion. The band at $1035\,cm^{-1}$ of the aromatic ring of the bisphenol is not affected by the curing reaction and it was used as a reference.

$$\alpha = 1 - \frac{\left(\frac{Abs_{915\,cm^{-1}}}{Abs_{1035\,cm^{-1}}}\right)_t}{\left(\frac{Abs_{915\,cm^{-1}}}{Abs_{1035\,cm^{-1}}}\right)_{t=0}} \quad (1)$$

2.2.2. Gel Formation (Gelation Process)

Another parameter used for the characterization of the materials in this research was the gelation period. During the curing process of a thermostable polymer, the glass transition temperature, T_g, increases as its molecular weight increases. As a consequence, a reduction of the free volume of the epoxy groups and of the unreacted primary amines takes place, given that some chains remain trapped in the infinite molecular weight networks. Gelation corresponds to the step that turns a viscous liquid into an elastic gel, taking place suddenly and irreversibly, which represents formation of infinite molecular weight molecules. This transition takes place at a specific conversion and within a certain time period. In epoxy-amine stoichiometrical amounts, having all the hydrogens the same reactivity, the theoretical gelation takes place at 58% of conversion [17].

As the reaction advances, the molecular weight of the polymer increases. The glass transition temperature is also affected, as it

increases with the degree of crosslinking from an initial T_{g0} value [18] to $T_{g\infty}$, which is the curing temperature at which total conversion is reached.

Gel times can be determined by different techniques. A texturometer fitted with a previously rated gauge was used. The gel time was reached when the gauge uses 0.2 N load to go inside and outside the material. The equipment used to determine the gel time was a TA-XT2i Texturometer (Stable Micro Systems LTd, Surrey, UK), using a 50 g mixture sample.

2.2.3. Dynamic Mechanical Thermal Analysis (DMTA)

Dynamic mechanical measurements were employed to determine variation of properties such as glass transition temperature, crystallinity, polymer crosslinking degree [19], and the storage modulus. DMTA is one of the most widely used techniques to study the influence of the molecular structure on the physical properties of polymers. It allows the study of the structure and mechanical properties of the viscoelastic solids and liquids through their dynamic and storage moduli. Storage modulus (E′) measures the energy stored during a sinusoidal cycle. The loss factor [$\tan\delta$, Eq. (2)] is defined as the ratio of the loss modulus (E″) to the storage modulus per cycle in the material and is defined as the tangent of the phase angle:

$$\tan\delta = E''/E' \tag{2}$$

The peak in the loss factor is associated with the highest damping of the polymeric structure. Therefore, small groups and chain segments can move. This happens close to T_g [20]. Damping is low when the polymer is below T_g, recovering the energy that is stored in the deformation when stress is removed. In that case, E″ is very small, as opposed to E′, and $\tan\delta < 1$. The industrial interest in DMTA focuses on the knowledge of the T_g of the material and in its long term behavior [18]. It is the most important parameter to indirectly determine average lifetimes, chemical degradations, etc.

Dynamic mechanical measurements were carried out in Rheometric Scientific DMTA Mk III equipment (TA Instruments, Newark, DE, USA) using a temperature range of 0–140°C at a frequency of 1 Hz and with a heating rate of 5°C/min. Rectangular test samples of approximately $30 \times 12.5 \times 2\,mm^3$ were used. A pre-established displacement of $\pm 32\,\mu m$ was used in all samples, using a bending mode in a simple cantilever. The apparatus included a 2 mm free length frame in which the sample was clamped while being subjected to a sinusoidal movement. The clamping method was always the same, tightening the bolts with a coupling torque of 10 N · m. All tests

were done in dry nitrogen to ensure that no moisture remained inside the apparatus.

2.2.4. Confocal Microscopy

The curing of the filled epoxies was also monitored by confocal microscopy. This technique uses point illumination and a pinhole in an optically conjugate plane in front of the detector to eliminate out-of-focus information. As only one point is illuminated at a time in confocal microscopy, 2D or 3D imaging requires scanning over a regular raster (*i.e.*, a rectangular pattern of parallel scanning lines) in the specimen. The confocal laser microscope that was used is a DM IRBE2 microscope (LEICA, Deerfield, IL, USA), with a clear field in transmitted and fluorescent incident light and an optical fitting for interferential contrast. It includes three fluorescence filters.

In order to monitor the curing process of the adhesive in the composite material, 1% (by wt.) fluorescein was added to render the material fluorescent. Monitoring was done by taking images every 3 min for 30 min and after that, every 15 min for 60 min.

2.3. Mechanical Properties

The mechanical properties were evaluated during the second part of this research work. Dry wear tests were carried out at room temperature using a pin-on-disk tribometer (Microtest, Madrid, Spain). A 6 mm diameter alumina ball was used for the pin. The test conditions were 180 rpm, with an applied load of 15 N, and relative humidity below 30%. The sliding distance was 1000 m. Wear was evaluated by volume loss (weight loss divided by the density of the material) and by the applied load and the sliding distance. Strength was evaluated by means of three-point bending tests and Shore D hardness measurements. In order to carry out three-point bending tests, rectangular specimens were manufactured. Afterwards, wear tracks as well as the fracture surface of the specimens were studied by SEM.

3. RESULTS

3.1. Infrared Spectroscopy

The IR spectra of the resin and hardener before mixing are shown in Fig. 2. Normally commercial epoxies are not pure but in fact mixtures of different components. The IR spectrum of the hardener shows that it is formed by primary amines because two stretching peaks appear at 3360 and 3297 cm^{-1}. The peaks lying between 1607 and 1508 cm^{-1} can be assigned to the C-C bond of the aromatic ring, to the NH bending

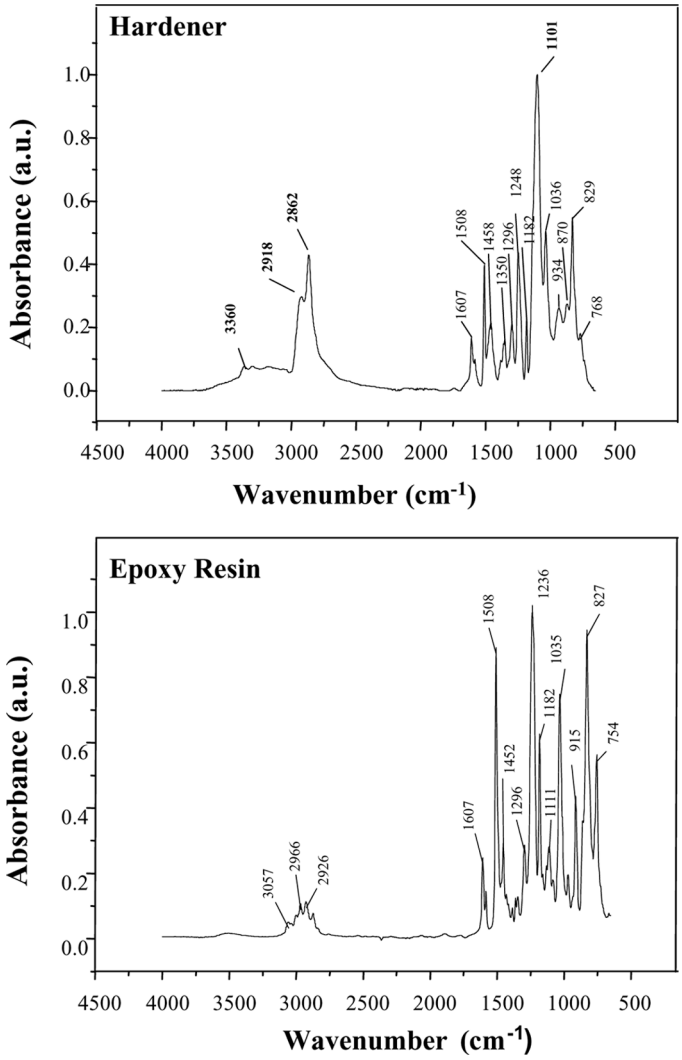

FIGURE 2 Infrared spectra of the hardener and resin before mixing.

vibration, and to the C=O stretching vibration. The peaks at 2918 and 2862 cm^{-1} correspond to C–H stretching of CH_2 groups, and that at 1458 cm^{-1} represents the C–H bending of the CH_2 groups. The hardener also shows the characteristic of C–O–C bands, symmetric stretching vibration at 1036 cm^{-1}, and asymmetric stretching vibration at 1101 cm^{-1}.

Assignment of the bands [21] for the resin (before curing, Fig. 2) can be observed in Table 2. The characteristic groups of the oxirane in the epoxy resin are located at 1035 and 915 cm^{-1}, both of which were used in this study to monitor the curing process. Apart from these bands, the aromatic =C-H stretching band can be observed at 3057 cm^{-1}, overlapping with the stretching C-H bands of the methyl group and of the terminal methanols. Asymmetric and symmetric stretching interactions of the methyl and methanol appear at 2966 and 2926 cm^{-1}, respectively, and the stretching vibration of the methyl and scissor stretching of the methanol appear at 1452 cm^{-1}. At 1607 and 1508 cm^{-1}, the stretching bands of the aromatic ring appear. Asymmetric stretching of the oxirane group corresponds to the band at 1296 cm^{-1}, although this band can also correspond to the wagging/bending vibration of the OH group. Stretching of the C-H link in the plane and out of the plane at 827 cm^{-1} can also be observed at 1183 cm^{-1}, both corresponding to the aromatic ring. Finally, the band at 1112 cm^{-1} corresponds to the stretching vibration of the alcohols and the band at 760 cm^{-1} is typical of the diglycidyl ether structure of an epoxy.

TABLE 2 Assignment of the Most Characteristic IR Bands of the Uncured and Cured Epoxy Resin

Wavenumber (cm^{-1})	Assignment (uncured epoxy)	Assignment (cured epoxy)
3419		-OH st
3057	ArC-H st, C-H st oxirane	ArC-H st, C-H st oxirane
2966–2926	$-CH_3$, $-CH_2-$ st	$-CH_3$, $-CH_2-$ st
2066–1890		ArC-C armonics
1607	ArC-C	ArC-C
1508	ArC-C	ArC-C
1452	$-CH_3$ δ as, $-CH_2-$ δ	$-CH_3$ δ as, $-CH_2-$ δ
1361		$-CH_3$ δ st
1296	C-O-C st as, oxirane ϖ CH_2, t CH_2	C-O-C st as, oxirane ϖ CH_2, t CH_2
1236	ArC-O-C-al st as	ArC-O-C-al st as
1182	ArC-H δ ip	ArC-H δ ip
1111	C-OH st	C-OH st
1035	ArC-O-C-al st s	ArC-O-C-al st s
915	C-O-C st s, oxirane	C-O-C st s, oxirane
827	ArC-H δ oop	ArC-H δ oop
754	$-CH_2$ γ, for C-(CH_2)n-C $n < 4$	$-CH_2$ γ, for C-(CH_2)n-C $n < 4$

st: stretching, Ar: aromatic, δ: bending, s: symmetric, as: asymmetric, ϖ: wagging, t: twisting, al: aliphatic, ip: in plane, oop: out of plane bending, γ: skeleton vibrations, n: number of CH_2 groups.

During the polymerization reaction of an epoxy-amine system, the active hydrogens from the amine react with the epoxy group, opening it. Most research indicates that this reaction mainly takes place through two simultaneous paths, one being not catalyzed and the other one catalyzed by OH groups generated in the reaction [22,23]. The degree of polymer crosslinking can be determined by formation of tertiary amines [24]. Other authors have used the infrared absorption band close to the epoxy group (4530 cm^{-1}) and the primary amine (4937 cm^{-1}) for calculation of crosslinking [2,25]. Since the wavenumber range used in this study was 400–4000 cm^{-1}, it was not possible to monitor the evolution of these peaks.

The infrared spectrum of the cured epoxy shows the characteristic peaks of an epoxy, as can be observed in Fig. 3. The assignment of the bands is shown in Table 2. Similar bands for the uncured resin (Fig. 2) are obtained and only two new weak bands appear: one corresponding to harmonics (at 2066 and 1890 cm^{-1}) and the symmetric stretching vibrations of the methyl at 1361 cm^{-1}. Apart from this, the OH stretching band corresponding to the hydroxyl group is shifted to a higher wavenumber due to the creation of hydrogen bond interactions.

Figure 4 shows an enlarged IR spectrum of the zone corresponding to the bands that were used to monitor the epoxy curing process. Disappearance of the peak corresponding to the oxirane (915 cm^{-1}) was monitored as well as the peak at 1035 cm^{-1} that corresponds to stretching of the bisphenol aromatic C-H link in the ring. The degree

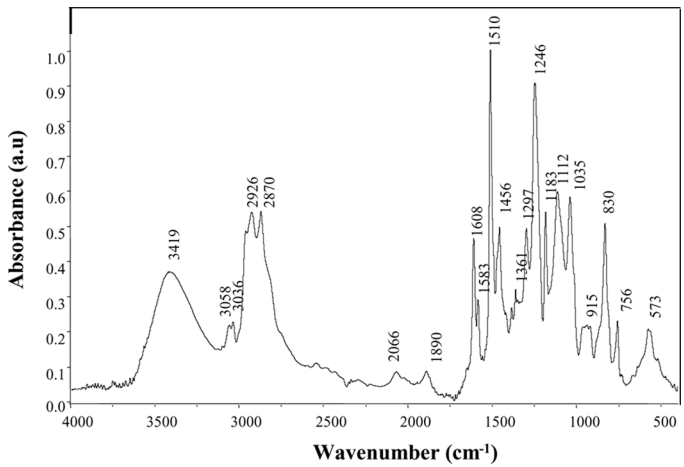

FIGURE 3 Infrared spectrum of the epoxy 9843 after cure (12 h).

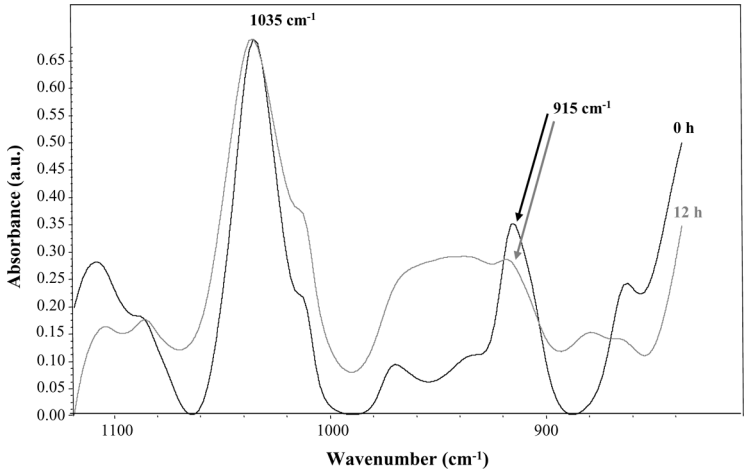

FIGURE 4 Enlarged infrared spectra of the epoxy before cure (0 h) and of the epoxy after cure (12 h).

of conversion of epoxy upon curing is obtained by applying Eq. (1). The variation of the degree of conversion as a function of time is given in Fig. 5a. The degree of conversion ranges between 85 and 95%. Addition of B_4C, in general, increased the degree of conversion, except when 6% of the 7 μm B_4C was added, in which the degree of conversion was slightly lower. The highest percentage was obtained for 6% of the 23 μm B_4C. The degree of conversion for additions of 12% was very similar and slightly superior to that of the epoxy without reinforcement. The differences found were very slight and did not follow a definite pattern. The epoxy containing 12% B_4C (23 μm) showed a faster reaction in such a way that 90% conversion was reached in only 30 min.

However, when studying the reaction for shorter time periods, that is to say the degree of conversion in the first hour of reaction, then major differences were observed between the different materials. In Fig. 5b it can be observed how the B_4C of 7 μm accelerates the reaction at the beginning, acting like a catalyst. In this case, a curing of almost 40% was obtained within the first 15 min, after which the reaction started to slow down. For a higher percentage of particles more conversion was obtained, reaching 57% for the epoxy with 12% of the 7 μm B_4C and 49% for the epoxy with 6% of the 7 μm B_4C, after a 1 h reaction (Fig. 5b).

Addition of 23 μm B_4C particles delays the epoxy curing reaction (Fig. 5b). The degree of conversion was 2% at 15 min for the epoxy with

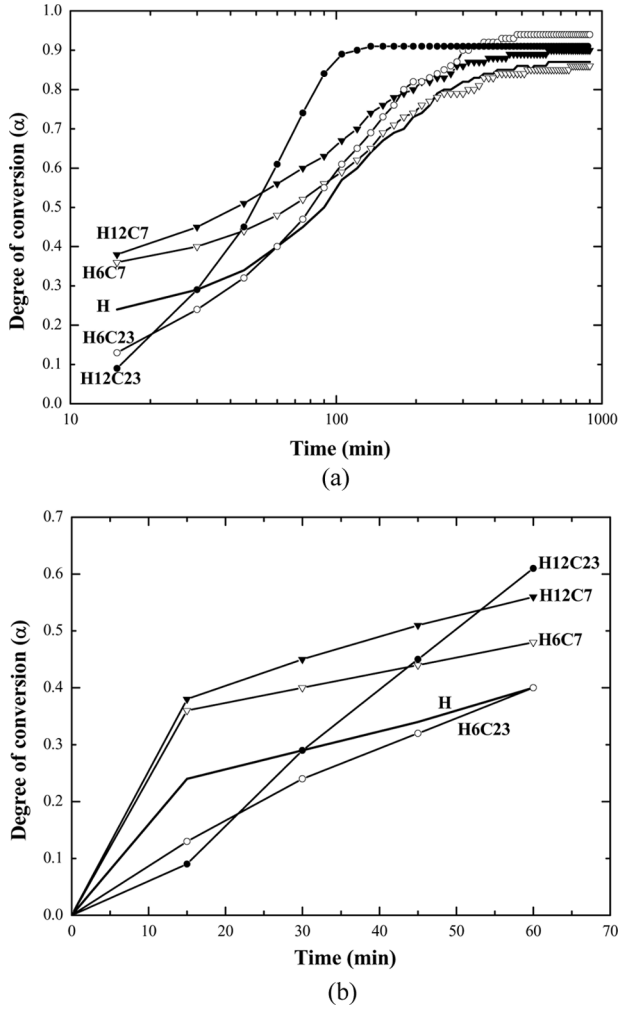

FIGURE 5 (a) Influence of the amount and particle size of B_4C in the degree of conversion as a function of time (logarithmic scale). (b) Detail of degree of conversion of the materials during the first hour of reaction.

12% B_4C, while the degree of conversion was 12% for a 6% addition. However, the base epoxy showed 28% degree of conversion after 15 min. Once the reaction started, 6% additions of 23 μm B_4C increased the degree of conversion almost linearly up to 1 h. With the same particle size and 12% B_4C, the reaction was very fast, reaching superior curing in relation to the base material within 1 h. At first, 23 μm

B_4C delayed the reaction and then acted as a catalyst, increasing the speed of reaction.

All low particle size B_4C additions acted as catalysts (Fig. 5b). The OH groups generated in the polymerization reaction also did [24,26], increasing the initial reaction rate. Equation (3) showed the catalytic process produced by OH. In the first stages, the concentration of the OH groups is scarce and the B_4C acts as a catalyst. The amount of OH groups increases as the reaction advances, becoming the main catalyst of the reaction. This effect is observed in Fig. 5b, where epoxy with 7 μm B_4C and the base epoxy have the same kinetic mechanism, although the conversion rates are different.

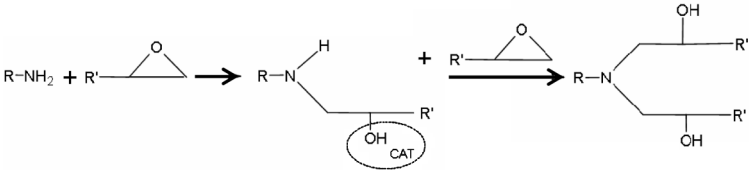

(3)

However, when 23 μm B_4C particles are added, their effect on the epoxy curing is exactly the opposite, delaying the reaction, to a greater extent by increasing the B_4C amount. Because of their particle size, a hindrance by the B_4C is produced, inhibiting the catalytic behaviour of 23 μm B_4C. The OH groups that act as a catalyst are formed as the reaction advances. In the end, the degree of conversion is similar in all the materials.

3.2. Gelation

In theory, gel time is reached at a degree of conversion of approximately 58% [19]. Figure 6 compares times to get to 58% conversion from FTIR spectroscopy and gel time. The gel time values obtained in this study are reached below the degree of conversion of 58%. It can be observed (Fig. 6) that 6% B_4C, independent of the particle size, considerably reduced the gel time, although additions of 12% practically maintained the time with respect to the epoxy alone. Particle size has no effect in this material property for the cases studied here.

There is an opposite trend in the variation of time at which 58% degree of conversion is reached (IR spectroscopy) and the gel time values of the reinforced epoxies (Fig. 6). Both the lowest times at 58% degree of conversion and the highest gel time values correspond to the epoxies containing 12% B_4C. This different trend can be explained by considering the two different techniques used. In the

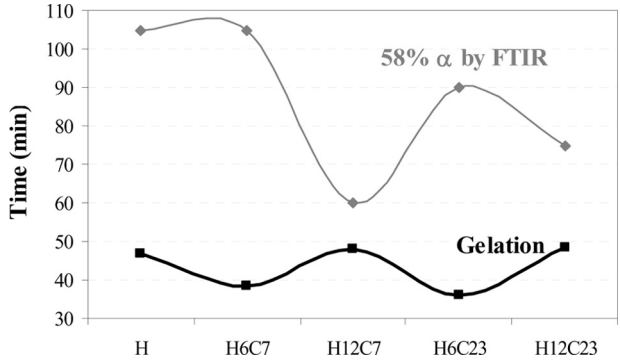

FIGURE 6 Variation of the gel time for the epoxy with different amounts and particle size of B_4C.

gel time measurement, the amount of adhesive mixture is critical as the noticeable heat evolved during curing facilitated the kinetics of polymerization. On the other hand, the friction caused by the cylindrical probe may also increase the heat and, therefore, the kinetics of the curing reaction. Therefore, the gel time values measured should be lower than those obtained by IR spectroscopy where friction is absent and heat evolved is much lower (a tiny amount of adhesive mixture, *i.e.*, a drop, is used).

3.3. Confocal Microscopy

Figure 7a displays 3D images obtained with confocal microscopy. It can be observed how the B_4C particles move to the bottom of the epoxy because of its low viscosity, apart from depositing and agglomerating. The greater density of the B_4C with respect to the epoxy is also an important factor in the precipitation effect of the B_4C particles. Mobility and agglomeration of the B_4C particles are independent of the initial dispersion; dispersion is good at zero time period (just after mixing), as shown in the 2D image in Fig. 7b.

The size and percentage of the particles do not influence their mobility. After 60 min, viscosity has increased enough to reduce the mobility of the particles.

3.4. Dynamic Mechanical Thermal Analysis (DMTA)

The glass transition area can be clearly distinguished in Fig. 8, with observed peaks in the curves corresponding to tan δ and E″, apart from a sudden drop in the value of storage modulus (E′).

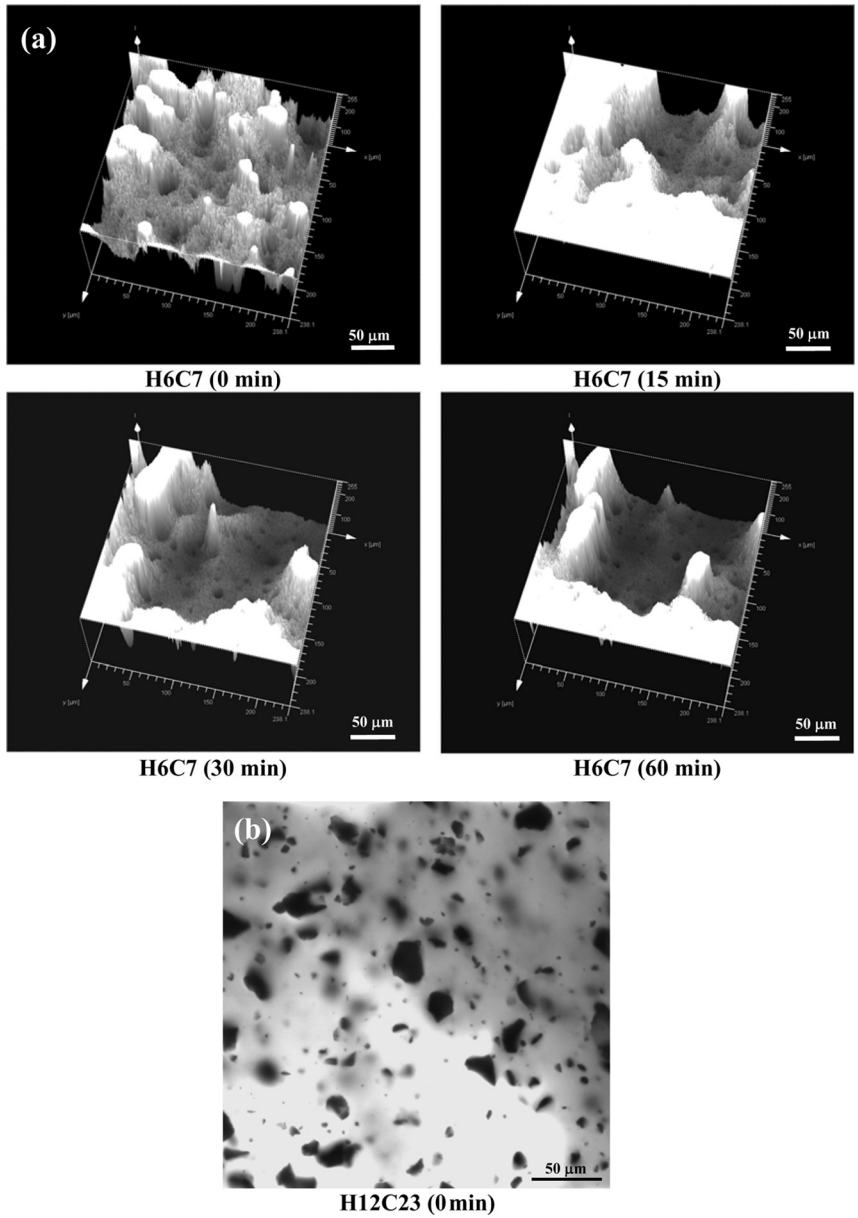

FIGURE 7 (a) 3D images of confocal microscopy for epoxy + 6% of the 7 μm B_4C at different curing times. (b) 2D image of confocal microscopy of epoxy + 12% of the 23 μm B_4C just after mixing. (The grey areas appear green in the microscope because of the fluorescein).

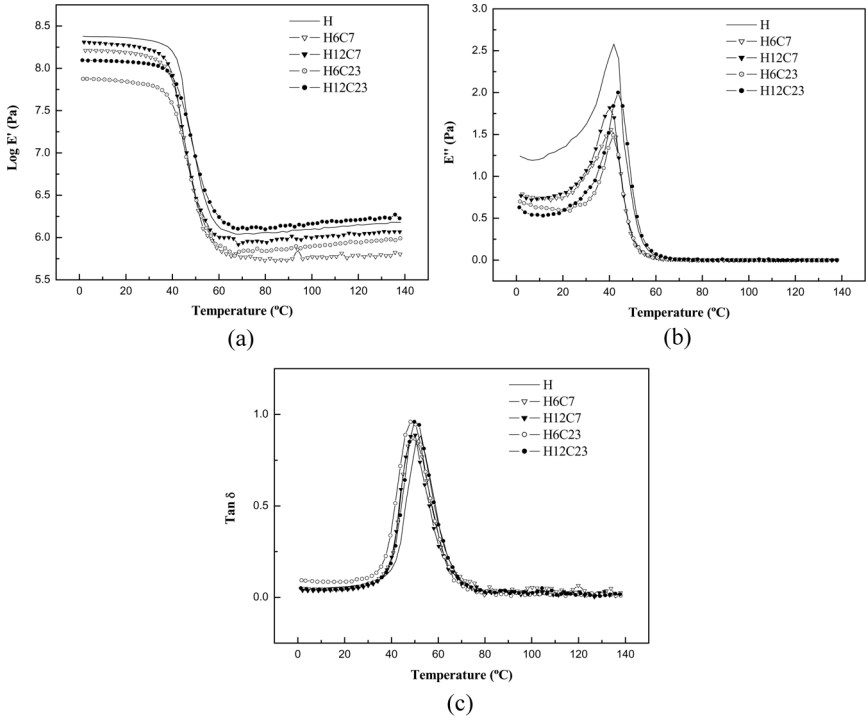

FIGURE 8 Variation for the different materials as a function of temperature of: (a) the storage modulus, (b) the loss modulus, and (c) tan δ.

The glass transition temperature can be considered as the middle point of the transition in log E′ (Fig. 8a) or the maximum in E″ or tan δ (Figs. 8b and 8c). The glass transition temperature obtained from the tan δ curve is the most employed criterion [27]. It is also quite common to use the E″ peak, although the glass transition temperature tends to be 20–30°C lower than that given by tan δ [28].

If the peak of the loss modulus is used (Fig. 8b), the values of T_g are slightly lower than those found with tan δ (Fig. 8c and Table 3). For the base epoxy, a value of 41.9°C (Fig. 8b) was obtained using the loss modulus and 52.5°C was obtained using tan δ (Table 3).

The storage modulus (Fig. 8a) in the glassy region is slightly lower for filled epoxy materials. The storage modulus data are not fully in agreement with the values corresponding to the degree of cure found by FTIR spectroscopy that shows slightly better degrees of cure in filled materials. This could be related to the stress accumulation that B_4C particles create in the material. In the rubbery region, the T_g of

TABLE 3 Some Parameters of the Plain Epoxy and B_4C-Epoxy Composites Cured at Room Temperature for 12 Hours (DMTA Experiments)

Material	Log E′ (25°C) [Pa]	Area (under tan δ peak) [a.u.]	Tg [°C] by tan δ	Log E′ (100°C) [Pa]
H	83.48	17.78	52.5	6.09
H6C7	81.74	19.71	49.2	5.77
H12C7	82.52	17.85	50.2	6.00
H6C23	78.21	21.63	48.2	5.89
H12C23	80.67	19.53	49.8	6.16

the reinforced materials are also below the base material, with the exception of the epoxy with 12% of 23 μm B_4C. The only filled epoxy with a straight rubbery plateau is the epoxy with 6% reinforcement (7 μm), while the remaining materials have a storage modulus that slightly increases with temperature. This is in agreement with the residual energy in the filled epoxy, thus making post-curing necessary in order to reach optimal mechanical properties.

If the loss modulus is analyzed (Fig. 8b), all the materials also have a modulus that is inferior to the unfilled epoxy and the peak of the curve appears at lower temperature.

According to Fig. 8c and Table 3, the T_g values of the reinforced materials are lower than for the unreinforced epoxy and no clear influence of the reinforcement particle size nor its content can be distinguished. Although the differences are not substantial, it is clear that B_4C particles hinder growth and crosslinking of the polymer chains. Crosslinking of the epoxy resin takes place during the curing reaction, forming a 3D network bonding molecular chains through covalent links. The more crosslinked the polymer is, the lower its molecular mass between crosslinking points and the greater its crosslinking density. As the number of crosslinking points increases, the mobility of the chains decreases [29], losing a certain amount of free volume (less viscous material) and the T_g increases. The greater the molecular movements associated to the transition, the greater the intensity of the peak in tan δ [30]. Hence, with a reduction of the molecular movements that are allowed, the intensity of the peaks in tan δ tends to diminish. The B_4C reduces the energy necessary to cause rotations around molecular bonds, thus originating a glass transition shift to lower temperatures. The same effect has been found with diluents [31], in which a decrease in T_g and tan δ signal is observed as the diluent content increases. However, an unexpected increase of the area under the tan δ peak (in the tan δ *vs.* temperature plot, Fig. 8c) with B_4C additions is found (Table 3). This is related to the unreacted

epoxy groups due to the presence of reinforcement. Those unreacted groups do not have restricted molecular movements and the area of the peak increases. On the other hand, the height of the $\tan\delta$ peak is very close to 1 in all reinforced epoxies with 23 μm B_4C particles, as the values of E' and E'' are very similar [Eq. (2)]. This could be related to short chain lengths in the epoxy due to high B_4C particle size.

3.5. Mechanical Properties

The physical and mechanical properties are shown in Table 4. Addition of 6% of B_4C particles to the epoxy does not produce changes in density. However, addition of 12% slightly reduces the density. This might be due to the increase of viscosity in the material before curing, making the filling of molds more difficult because of the low fluidity of epoxy with 12% B_4C.

The Shore D hardness values increase with the addition of B_4C particles (Table 4), with no difference being found either with the added percentage or with the particle size. It is known that the addition of abrasion-resistant particles significantly increases the hardness of composites. Hardness should also increase with the particle size and wear should decreases [32,33]. In this research, wear increases with the addition of particles. This increase is greater in the case of 12% additions of 23 μm particles. The reason is the lack of anchoring of the particles by the epoxy, a gap being found between resin and B_4C (Fig. 9, black circle). In this case, the particles act as a third body, increasing abrasive wear. Logically, a high number of particles and high particle size are two factors that influence this value (Table 4).

The friction coefficient also increases when particles are added, as in the case of wear. This is due to the increase in abrasive wear and the existence of B_4C particles in the wear track.

TABLE 4 Physical and Mechanical Properties of Plain Epoxy and B_4C-Epoxy Composites

Material	Relative density (%)	Hardness (Shore D)	Bending strength (MPa)	Elongation at break (%)	Wear (mm^3/Nm) 10^{-4}	Friction coefficient
H	98 ± 1	75 ± 1	102 ± 3	5 ± 1	8 ± 1	0.40 ± 0.05
H6C7	99 ± 1	79 ± 2	99 ± 4	7 ± 2	14 ± 1	0.48 ± 0.05
H12C7	96 ± 2	78 ± 3	113 ± 2	6 ± 2	11 ± 1	0.42 ± 0.05
H6C23	98 ± 1	79 ± 1	95 ± 3	6 ± 1	11 ± 1	0.47 ± 0.05
H12C23	94 ± 3	78 ± 2	109 ± 1	7 ± 3	20 ± 2	0.57 ± 0.05

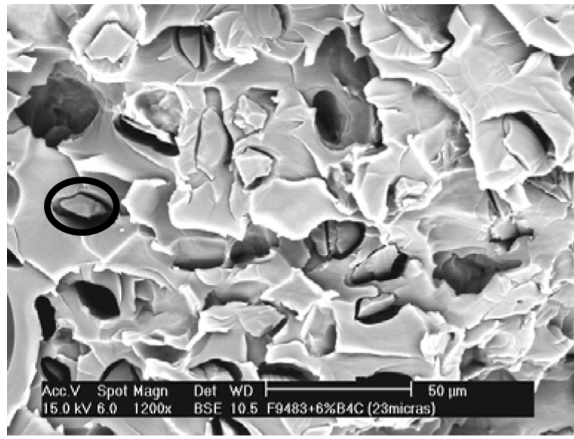

FIGURE 9 SEM micrograph corresponding to the fracture surface of the epoxy with 6% B_4C (23 µm).

The influence of B_4C particles in the bending strength and elongation at break is quite important, given that B_4C is a ceramic material with a high mechanical strength, although it is very brittle. However, in Table 4 it can be seen that the values calculated for these materials are very similar. Addition of 6% B_4C reduces the strength for both particle sizes. However, an addition of 12% increases the strength. Two opposing effects are found: the beneficial effect of adding ceramic particles on the one hand and the detrimental effect of the shape of the particles on the other (Fig. 1). The polygonal shape of the particles, with great sharp edges, makes them act as crack promoters in the material, increasing stresses and thus reducing strength.

There is not a meaningful influence of B_4C addition on elongation at break, as error bars are overlapped (Table 4). This particular epoxy is brittle and its brittleness does not change with addition of ceramic material.

The determination of the different mechanical properties was completed with a SEM study of the wear tracks and fracture surface of the materials. Since B_4C is a hard material [3,4], it acted as an abrasive and produced alumina pin wear. Ball wear left alumina in the wear track, which was not observed in the epoxy without B_4C.

Plain epoxy presents abrasive wear. Some epoxy detached particles stick along the track edges (Fig. 10a, white circle). Measured wear is low due to scarce mass loss, although the wear track is deep and wide. B_4C addition increases wear (Table 4), since it constitutes another abrasive element. B_4C and alumina particles are found in the track (Fig. 10b, black circle for alumina and white circle for B_4C particle).

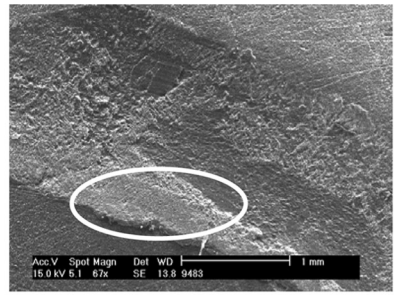

(a) H
White circle: detached and stuck epoxy particles

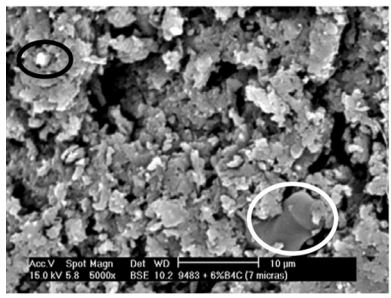

(b) H6C7 (B_4C detail)
White circle: B_4C particle
Black circle: alumina particle

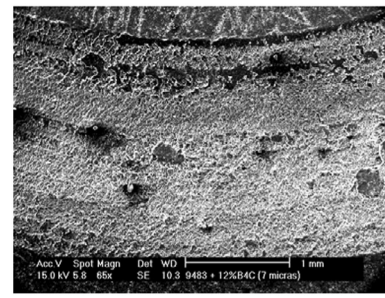

(c) H12C7

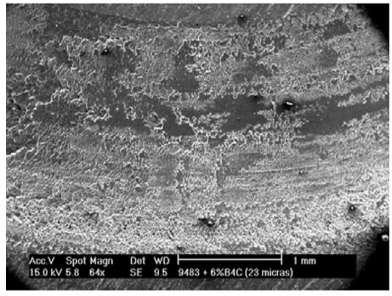

(d) H6C23

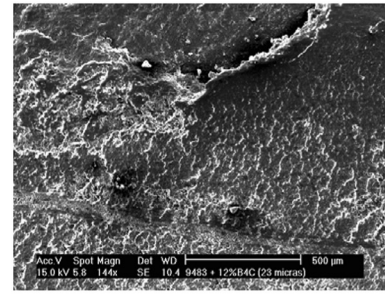

(e) H12CB23

FIGURE 10 SEM micrographs of wear tracks of manufactured epoxy-B_4C composites.

Micrographs indicate that great differences do not exist between wear tracks, neither with the particle size (Fig. 10c and 10d) nor with the amount of carbide. The composite with the highest B_4C content and largest particle size presents the highest wear values (Table 4) and the wear track presents great bursts of material (Fig. 10e). The wear

tracks of the composite materials do not present adhered particles, and they are free of grooves or deformations. Those wear tracks present less depth than those found in plain epoxy, but the absence of particle adhesion gives higher mass losses. The adhesion of ceramic particles to epoxy could be improved through a surface treatment, such as silane coatings on SiC microparticles [34] and nanoparticles [35], improving the mechanical properties of the composite.

4. CONCLUSIONS

This work analysed the influence of B_4C additions on the curing process and mechanical properties of an epoxy resin. The following main conclusions were obtained:

1. Addition of B_4C did not affect the degree of conversion of the epoxy during curing. It acted as an accelerator or retardant of the reaction kinetics during the first hour, depending on particle size and the amount of added carbide.
2. Given the low viscosity of the epoxy and the long curing time, the particles were deposited and tended to agglomerate until gelation was produced. This gel time oscillated between 50 and 100 min, depending on the technique employed in its quantification and on the material.
3. Addition of B_4C shifted the glass transition temperature of the epoxy to lower values.
4. Epoxy-B_4C composites showed excellent bending strength, increasing with B_4C content and with the smaller particles.
5. Due to a lack of adhesion between the B_4C particles and the epoxy, the particles acted as a third body during wear tests, increasing abrasive wear of the material.

ACKNOWLEDGMENTS

The authors wish to acknowledge the Adhesion and Adhesives Laboratory of the University of Alicante, University Carlos III Foundation of Madrid, and the Technological Institute of Chemistry and Materials "Álvaro Alonso Barba" for their financial support.

REFERENCES

[1] Okuno, K., *Radiat. Prot. Dosim.* **115**, 258–261 (2005).
[2] Prades, P., Pazos, M., Gonzalez, G., López, A., and Paz, S., *Química e Industria* **46**, 288–290 (1999).

[3] Thevenot, F., *J. Eur. Ceram. Soc.* **6**, 205–225 (1990).
[4] Lazzari, R., Vast, N., Besson, J. M., Baroni, S., and Dal Corso, A., *Phys. Rev. Lett.* **83**, 3230–3233 (1999).
[5] Ahn, H. S., Cuong, P. D., Shin, K. H., and Lee, K. S., *Wear* **259**, 807–813 (2005).
[6] Zorzi, J. E., Perottoni, C. A., and da Jornada, J. A. H., *Mater. Lett.* **59**, 2932–2935 (2005).
[7] Shiway, P. H. and Hutching, I. M., *Wear* **149**, 85–98 (1991).
[8] Lee, H. and Séller, R. F., *J. Amer. Ceram. Soc.* **86**, 1468–1473 (2003).
[9] Barney, W. K., Shemel, G. A., and Seymour, W. E., *Nucl. Sci. Eng.* **1**, 439–448 (1958).
[10] Dzhosyuk, S. N., Matón, C. E. H., Mckinsey, D. N., Thompson, A. K., Yang, L., Doyle, J. M., and Huffman, P. R., *Nucl. Instrum. Meth. B* **217**, 457–470 (2004).
[11] Harrison, C., Burgett, E., Hertel, N., and Grulke, E., *Space Technology and Applications International Forum Conference Proceedings*, (University of New Mexico, Alburquerque, 2008), Vol. 969, pp. 484–491.
[12] Sund, R. E. and Walton, R. B., *Phys. Rev.* **146**, 824–835 (1966).
[13] Lee, C. H., Park, J., Choi, B. H., Oh, H., and Han, Y. S., *Development of Neutron Shielding Block by Epoxy Molding*, (Korea Atomic Energy Research Institute, Taejon, Republic of Korea, 2001).
[14] Henkel Adhesivos y Tecnologías, S.L. Technical Datasheet (http://tds.loctite.com/tds5/docs/9483-ES.PDF).
[15] Avella, M., Errico, M. E., Martelli, S., and Martuscelli, E., *Appl. Organomet. Chem.* **15**, 434–439 (2001).
[16] Dennis, H. R., Hunter, D. L., Chang, D., Kim, S., White, J. L., Cho, J. W., and Paul, D. R., *Plast. Eng.* **1**, 56–60 (2001).
[17] Flory, P. L., *Principles of Polymer Chemistry,* 15th ed., (Cornell Univ. Press, Ithaka, USA, 1992).
[18] Turi, C. A., *Thermal Characterization of Polymeric Materials*, (Academic Press, San Diego, 1981).
[19] Wilson, A. D., Nicholson, J. W., and Prosser, H. J., *Surface coatings-1*, (Elsevier Applied Science, London, 1987).
[20] Nielsen, L. E. and Landel, R. F., *Mechanical Properties of Polymer and Composites,* 2nd ed., (Marcel Dekker, New York, 1994).
[21] Pretsch, E., Bühlmann, P., and Affolter, C., *Structure Determination of Organic Compounds*, (Springer-Verlag, Berlin, 2000).
[22] Sourour, S. and Kamal, M. R., *Termochim. Acta* **14**, 41–59 (1976).
[23] Riccardi, C. C., Adabbo, H. E., and Williams, R. J. J., *J. Appl. Polym. Sci.* **29**, 2481–2492 (1984).
[24] Paz-Abuín, S., López-Quintela, A., Pazos-Pellín, M., and Paz-Pazos, M., *Polymer* **38**, 3795–3804 (1997).
[25] Mijovic, J., Andjelic, S., Winnie-Yee, C. F., Belluci, F., and Nicolais, L., *Macromolecules* **28**, 2797–2806 (1995).
[26] Horie, K., Hiura, H., Sawada, M., Mita, I., and Kambe, H., *J. Polym. Sci. A* **8**, 1357–1372 (1970).
[27] Ellis, B., *Chemistry and Technology of Epoxy Resins*, (Chapman and Hall, London, 1993).
[28] Hale, A., Macosko, C. W., and Bair, H. E., *Macromolecules* **24**, 2610–2621 (1991).
[29] Matsuoka, S., *Relazation Phenomena in Polymers*, (Carl Hanser Verlag, Munich, 1992).
[30] Miller, D. R. and Macosko, C. W., *Macromolecules* **9**, 206–211 (1976).
[31] Nuñez-Regueira, L., Villanueva, M., and Fraga-Rivas, I., *J. Therm. Anal. Cal.* **86**, 463–468 (2006).

[32] Axen, N. and Jacobson, S., *Wear* **174**, 187–199 (1994).
[33] Durand, J. M., Vardavoulias, M., and Jeandin, M., *Wear* **181–183**, 833–839 (1995).
[34] Abenojar, J., Del Real, J. C., Martínez, M. A., and Cano de Santayana, M., *J. Adhesion*, **85**, 287–301 (2009).
[35] Zhou, T., Wang, X., Mingyuan, G. U., and Liu, X., *Polymer* **49**, 4666–4672 (2008).